Type-1 cytokines regulate MMP-9 production and E-cadherin disruption to promote melanocyte loss in vitiligo

Nesrine Boukhedouni, Christina Martins, Anne-Sophie Darrigade, Claire Drullion, Jérôme Rambert, Christine Barrault, Julien Garnier, Clément Jacquemin, Denis Thiolat, Fabienne Lucchese, Franck Morel, Khaled Ezzedine, Alain Taieb, François-Xavier Bernard, Julien Seneschal, and Katia Boniface1

Graphical abstract

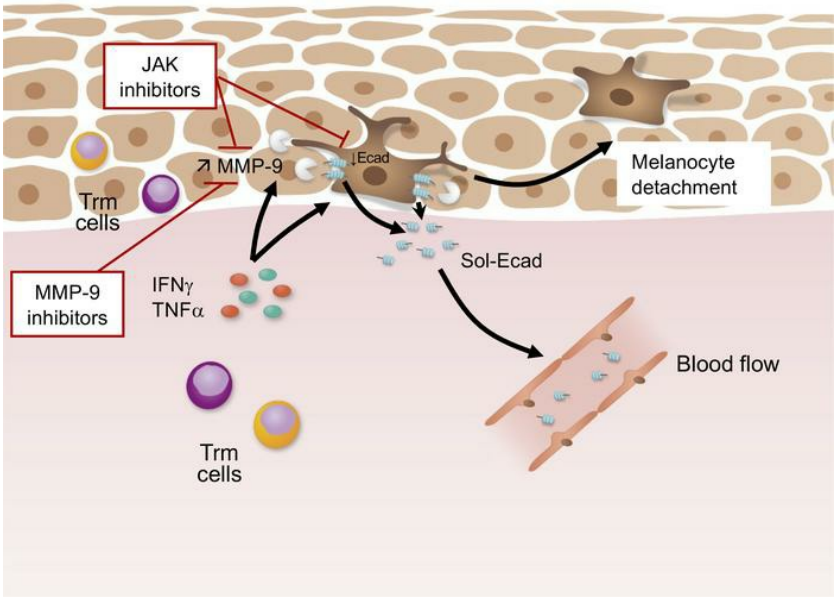

Loss of melanocytes is the pathological hallmark of vitiligo, a chronic inflammatory skin depigmenting disorder induced by exaggerated immune response, including autoreactive CD8 T cells producing high levels of type 1 cytokines. However, the interplay between this inflammatory response and melanocyte disappearance remains to be fully characterized. Here, we demonstrate that vitiligo skin contains a significant proportion of suprabasal melanocytes, associated with disruption of E-cadherin expression, a major protein involved in melanocyte adhesion. This phenomenon is also observed in lesional psoriatic skin. Importantly, apoptotic melanocytes were mainly observed once cells were detached from the basal layer of the epidermis, suggesting that additional mechanism(s) could be involved in melanocyte loss. The type 1 cytokines IFN-γ and TNF-α induce melanocyte detachment through E-cadherin disruption and the release of its soluble form, partly due to MMP-9. The levels of MMP-9 are increased in the skin and sera of patients with vitiligo, and MMP-9 is produced by keratinocytes in response to IFN-γ and TNF-α. Inhibition of MMP-9 or the JAK/STAT signaling pathway prevents melanocyte detachment in vitro and in vivo. Therefore, stabilization of melanocytes in the basal layer of the epidermis by preventing E-cadherin disruption appears promising for the prevention of depigmentation occurring in vitiligo and during chronic skin inflammation.

Introduction

Vitiligo is the prototype of a depigmenting disease due to an exaggerated skin immune response. However, depigmentation is not restricted to vitiligo and may occur during the course of other chronic skin inflammatory disorders, such as psoriasis (1). Vitiligo affects the quality of life of patients dramatically and therapies so far remain limited (2). Its pathological hallmark is the loss of epidermal melanocytes, the cells located in the basal layer of the epidermis and responsible for pigmentation and skin phototype. Vitiligo is a complex multifactorial disease combining genetic predisposition and environmental triggers (e.g., friction, chemicals), together with metabolic, immunologic, and inflammatory abnormalities (2, 3). Depigmentation in vitiligo is consistently associated with infiltration of immune cells, in particular CD8 T cells, in close apposition to the remaining melanocytes, at least during disease progression (4–6). Importantly, vitiligo should be viewed as an immune memory skin disease, as recently highlighted by the role of resident memory T cells (Trm) during pathogenesis (7–9). A prominent type 1 cytokines–skewed immune profile is characteristic of the skin of patients with vitiligo, as the majority of melanocyte-specific skin CD8 Trm cells express the chemokine receptor CXCR3 and produce elevated levels of the type 1–related cytokines IFN-γ and TNF-α (7, 10). The CXCR3/IFN-γ/TNF-α axis has been shown to be involved in the process leading to depigmentation in vitro and in vivo in a disease-prone mouse autoimmune model of vitiligo (11–14), and IFN-γ and TNF-α are involved in epidermal pigmentation homeostasis, inhibiting melanocyte function, phenotype, and melanogenesis (4–6, 15, 16). However, although previous studies identified the role of these cytokines in the pathomechanism of the disease, the interplay between inflammation and the melanocyte loss characterizing vitiligo remains elusive.

The leading hypothesis is that melanocyte loss is mediated by autoreactive CD8 T cells (3, 17–19). Indeed, in vitro studies reported that CD8 T cells isolated from the skin of patients with vitiligo induced the apoptosis of autologous melanocytes (17, 20, 21). Nonetheless, clear evidence of the presence of apoptotic cells in vivo is still lacking, and we recently showed that CD8 T cells from vitiligo skin display moderate cytotoxic activity comparable with that found in healthy skin and the lesional skin of patients with psoriasis (7), suggesting that additional disease mechanism could be involved in melanocyte disappearance. Moreover, depigmentation in mouse models of vitiligo depends rather on IFN-γ signaling, whereas perforin is dispensable (11, 13), suggesting that the release of proinflammatory cytokines such as IFN-γ in the skin is important in the process leading to depigmentation.

Melanocyte disappearance could also result from their detachment (22, 23). The stabilization of melanocytes in the basal layer of the epidermis is dependent on the adhesion protein E-cadherin (24, 25). Interestingly, impaired cell-surface E-cadherin expression was recently shown in the nonlesional skin of patients with vitiligo (26, 27). Several mechanisms could be involved in such a disruption, such as inhibition of its expression, internalization in the endosomal structure, or cell surface cleavage into a soluble form (soluble E-cadherin). E-cadherin cleavage may be induced by several proteases, including MMPs such as MMP-3, MMP-7, and MMP-9, A disintegrin, and MMP domain–containing protein 10 (ADAM10), which are all known to be involved in extracellular matrix remodeling and cell migration in various physiologic and pathologic processes (28, 29).

MMPs are a family of Zn-dependent proteases with common functional and structural properties. MMP-9, also known as 92kDa gelatinase/type IV collagenase, is constitutively expressed primarily in leukocytes, whereas most other cell types including keratinocytes express MMP-9 in response to various proinflammatory cytokines such as IFN-γ, TNF-α, IL-1β, and IL-6 (30, 31). Initially recognized for its collagen-remodeling function, MMP-9 activity is now known for its role in the control of immune responses, such as the migration of immunocompetent cells into and out of peripheral tissues, and the regulation of the activation of both CD4 and CD8 T cells (32–34).

Here we report that vitiligo perilesional skin is characterized by the basal detachment of melanocytes associated with the disruption of E-cadherin surface distribution and the release of soluble E-cadherin; melanocyte apoptosis was mainly noticed after their detachment from the basal epidermal layer. Strikingly, this phenomenon is not restricted to vitiligo disease but may also occur in psoriasis. We further show that the type 1 cytokines IFN-γ and TNF-α induce melanocyte detachment in both in vitro and in vivo models, and that this effect is dependent on the inhibition of E-cadherin gene expression, internalization of E-cadherin, and its cleavage through the release of MMP-9 by keratinocytes. Strikingly, MMP-9 inhibitors and JAK inhibitors prevented the release of soluble E-cadherin, leading to the stabilization of melanocytes in the basal layer of the epidermis. Our results highlight an additional disease mechanism that leads to the loss of melanocytes in vitiligo and more generally in skin inflammation, suggesting the need for further exploration of therapeutic strategies aiming to both dampen the inflammation and maintain melanocyte stability in the basal layer of the epidermis of patients with vitiligo.

Results

Detachment of basal melanocytes is a hallmark of vitiligo and psoriasis. We first used immunofluorescence to exam-ine the distribution of melanocytes in the epidermis in the context of skin inflammation. We examined the perilesional skin of patients with both vitiligo and psoriasis and the lesional skin of patients with psoriasis (Figure 1, A and B, patient characteristics are displayed in Supplemental Tables 1 and 2; supplemental mate-rial available online with this article; https://doi.org/10.1172/jci.insight.133772DS1). Psoriasis was used as the archetype of a skin inflammatory disease. Collagen VII staining was used to identify the basal layer of the epidermis. Whereas melanocytes were located in the basal layer of the epidermis in the control skin of unaffected individuals, a marked number of melanocytes were found in not only the suprabasal layers in the vitiligo perilesional skin of patients with stable or active disease but also the acanthotic epidermis of the perilesional skin of patients with concomitant psoriasis and vitiligo. Strikingly, similar observations were made in the lesional skin of patients only with psoriasis. The remaining melanocytes in vitiligo perilesional skin were unable to proliferate irrespective of their localization within the epidermis, unlike the proliferating melanocytes observed in lesional psoriatic skin, as revealed by Ki67 expression (Supplemental Figure 1). This suggests that while the detachment of melanocytes is a common process seen in vitiligo and psoriasis, vitiligo is characterized by the absence of melanocyte regeneration, unlike psoriasis. Importantly, cleaved caspase-3 staining or TUNEL assay showed that only few basal melanocytes were apoptotic in these conditions. This was in contrast with the epidermal cell death observed in cutaneous lupus erythematosus and toxic epidermal necrolysis, 2 skin diseases associated with strong inflammation and epidermal cell death (Figure 1, C and D and Supplemental Figure 2). Apoptotic suprabasal melanocytes were evidenced only in some patients with active vitiligo (Figure 1, C and D). This suprabasal localization of melanocytes in vitiligo and psoriasis skin seems to be the consequence of a defect in their adhesion to keratinocytes, as shown by the disrupted distribution of the major adhesion molecule mediating melanocyte adhesion to keratinocytes, E-cadherin (25), in both melanocytes and keratinocytes (Figure 1E).

Melanocytes were classified into 3 types according to the distribution of cell surface E-cadherin stain-ing, as previously described (26): homogeneous (type 1), heterogeneous (type 2), and absence of E-cadherin labeling (type 3). Compared with healthy control skin, in which melanocytes stained homogeneously for E-cadherin, melanocytes from vitiligo perilesional skin, particularly in the active phase of the disease, and lesional psoriasis skin displayed a discontinuous cell-surface E-cadherin expression (Figure 1E and Supple-mental Figure 3A). In addition, soluble E-cadherin levels were significantly higher in the sera of patients with stable and active vitiligo compared with those of healthy controls (Figure 1F). These findings suggest that proinflammatory factors released by immune and epidermal cells during skin inflammation are able to regulate the distribution of E-cadherin on melanocytes and are responsible for their detachment from the basal layer of the epidermis.

Type 1 cytokines IFN-γ and TNF-α induce detachment of melanocytes and disrupt E-cadherin distribution. The immune response of vitiligo is predominantly associated with Th1/Tc1 cells infiltrating the skin, together with an elevated production of both IFN-γ and TNF-α (3). This immune bias is also found to a lesser extent in psoriasis compared with the strong Th17-skewed immune profile (35).

We next used an in vitro 3D model of reconstructed pigmented human epidermis (RHPE) contain-ing both keratinocytes and melanocytes to investigate whether TNF-α and IFN-γ could be involved in the E-cadherin disruption observed in patients. We found that the combination of TNF-α and IFN-γ induced the detachment of more melanocytes from the basal layer than each cytokine alone. Such detachment was also observed in vitro on cocultures of melanocytes and keratinocytes (Supplemental Figure 3, B and C). The process was mediated partly by an altered E-cadherin distribution in melanocytes (Figure 2, A and B and Supplemental Figure 3D). It was not associated with prominent melanocyte cell death, as observed by TUNEL assay staining (Figure 2C) or by assessing melanocyte viability in response to increasing concentrations of these cytokines (Supplemental Figure 4). In addition, only the combination of TNF-α and IFN-γ was able to downregulate significantly the expression of the E-cadherin encoding gene CDH1. This inhi-bition was specific to melanocytes as CDH1 transcript levels were not regulated in keratinocytes (Figure 2D). The decrease was dose dependent and time dependent (Figure 2, E and F). TNF-α and IFN-γ also decreased transcript levels of the melanocyte adhesion–related genes CCN3 and DDR1, albeit more weakly, whereas no significant regulation of the β-catenin–encoding gene CTNNB1 was noted (Supplemental Figure 5). DDR1 was recently reported to stabilize the membrane localization of E-cadherin (36). Importantly, the 2 cytokines induced E-cadherin relocalization in melanocytes, as evidenced by the presence of E-cadherin in vesicular structures positive for LAMP-1 staining, a known marker for lysosomes and late endosomes (Figure 2G). Furthermore, levels of soluble E-cadherin were also increased in cell-free supernatants of RHPE treated by both TNF-α and IFN-γ (Figure 2H), suggesting their ability to induce cleavage of E-cadherin indirectly.

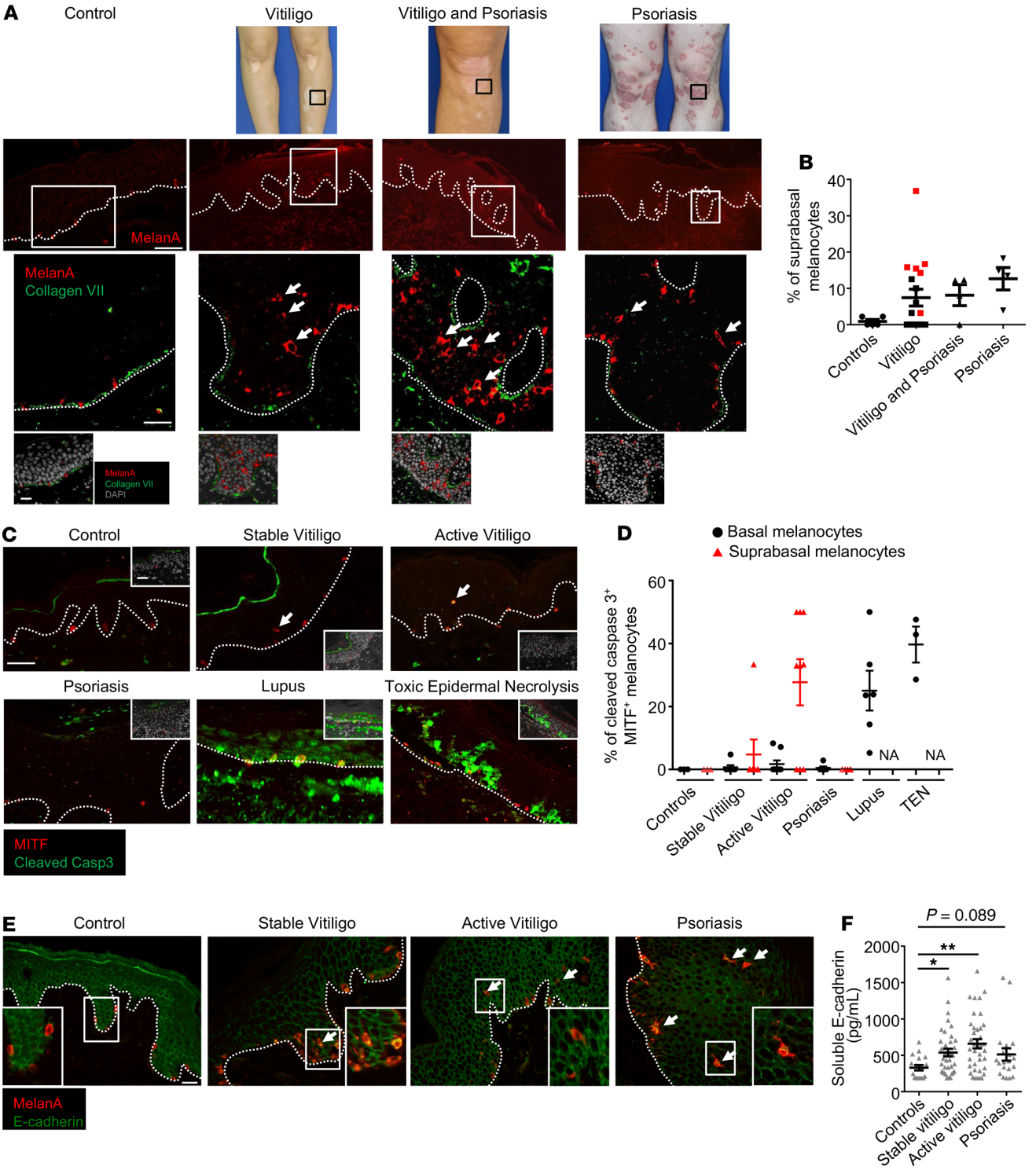

Figure 1. Melanocyte loss results from defective adhesion of melanocytes and not from apoptosis. (**A**) Representative immunofluorescence analysis showing melanocytes (red, Melan-A) and basal layer of epidermis stained with an anti–type VII collagen antibody (green) in control healthy skin, vitiligo perilesional skin, skin obtained from patients with concomitant vitiligo and psoriasis, and lesional psoriatic skin. Dashed lines repre-sent dermoepidermal layer. Arrows show suprabasal melanocytes in different conditions. Scale bars: 50 μm (top), 20 μm (bottom). (**B**) Proportion of suprabasal melanocytes in control healthy skin (n = 5), stable or active vitiligo perilesional skin (n = 18; black squares: stable vitiligo, red squares: active vitiligo), perilesional skin of patients with association of vitiligo and psoriasis (n = 4), and lesional psoriatic skin (n = 4). (**C**) Representative analysis of epidermal cell death using cleaved caspase-3 antibody (green). Melanocytes were stained with anti-MITF antibody (red) in control healthy skin, stable and active vitiligo perilesional skin, or lesional skin from psoriasis, cutaneous lupus erythematous, and toxic epidermal necrolysis. Dashed lines represent dermoepidermal layer. Scale bar: 20 μm. (**D**) Proportion of cleaved caspase-3$^+$ MITF$^+$ basal (circles) or suprabasal (triangles) melanocytes in control healthy skin (n = 3), stable (n = 4) or active vitiligo perilesional skin (n = 6), lesional skin of psoriasis (n = 6), cutaneous lupus erythematous (n = 6), and toxic epidermal necrolysis (n = 3). **(E)** Representative immunofluorescence analysis of expression of E-cadherin (green) and melanocytes (red, Melan-A staining) in control healthy skin, perilesional stable or active vitiligo skin, and lesional psoriatic skin. Staining is representative of 10 indepen-dent patients. Dashed lines represent dermoepidermal layer. Arrows identify suprabasal melanocytes. Scale bars: 50 μm (right) and 10 μm (left). **(F)** Assessment by ELISA of soluble E-cadherin levels in the sera of healthy controls (n = 18) or patients with stable (n = 37), progressive (n = 38) vitiligo, or psoriasis (n = 20). Data show mean ± SEM. *P < 0.05, **P < 0.01; calculated with a Kruskal-Wallis test.

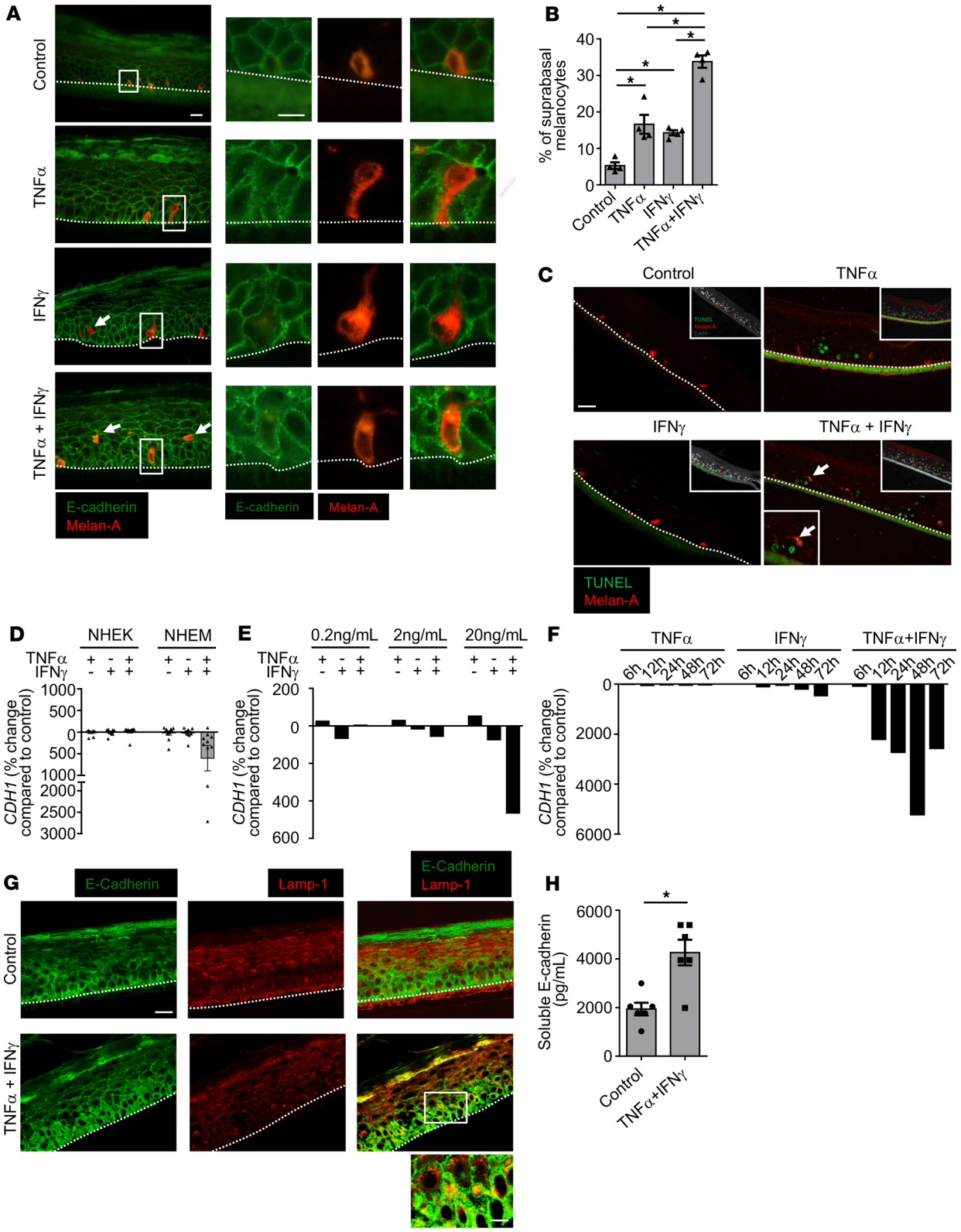

Figure 2. Combined activity of IFN-γ and TNF-α reproduces human vitiligo features in a 3D model of reconstructed pigmented epidermis in vitro. (**A**–**C**) Reconstructed human pigmented epidermis (RHPE) containing melanocytes were stimulated for 24 hours in the presence or absence of 10 ng/mL of TNF-α and IFN-γ, alone or in combination. (**A**) Representative immunofluorescence analysis of Melan-A (red) and E-cadherin (green) expression. Alteration of E-cadherin expression around melanocytes. Dashed lines represent dermoepidermal layer. Scale bars: 20 μm (left), 10 μm (right). (**B**) Proportion of suprabasal melanocytes in the different conditions (n = 4). (**C**) Representative analysis of epidermal cell death using a TUNEL assay (green); melanocytes were stained with anti-Melan-A antibody (red). Dashed lines represent the dermoepidermal layer. Scale bar: 20 μm. Staining is representative of 3 independent experiments. (**D**) Primary cultures of normal human epidermal keratinocytes (NHEK, left, n = 10) or melanocytes

(NHEM, right, $n = 11$) were treated for 24 hours with 20 ng/mL of IFN-γ and/or TNF-α. *CDH1* gene expression in epidermal cells was analyzed by real-time PCR. Results are shown as the percentage of change compared with the control culture. (**E**) Dose-response study of *CDH1* gene expression in NHEM after 24 hours stimulation with TNF-α and/or IFN-γ. (**F**) Kinetic analysis of *CDH1* gene expression in NHEM in response to 20 ng/mL of TNF-α and/or IFN-γ. Results from 1 experiment are shown in **E** and **F** and are representative of 4 independent experiments with 4 independent donors. *GAPDH* was used as a housekeeping gene. (**G**) Confocal microscopy analysis of RHPE treated in the presence or absence of the combination of 10 ng/mL of TNF-α and IFN-γ for 24 hours. Sections were stained for E-cadherin (green) and LAMP-1 (a marker for lysosomes and late endosomes, red). Merge shows the presence of E-cadherin molecule into LAMP-1 vesicle structures. Scale bars: 20 μm (top); 10 μm (bottom). Stainings are representative of 3 independent experiments. (**H**) Assessment by ELISA of soluble E-cadherin levels in cell-free supernatants of RHPE treated for 24 hours in the presence or absence of 10 ng/mL of TNF-α and IFN-γ. Data in **B**, **D**, and **H** show mean ± SEM. $*P < 0.05$, $**P < 0.01$; calculated with 2-tailed Mann-Whitney (**B**) or Wilcoxon (**H**) tests.

MMP-9 levels are increased in the circulation and skin of patients with vitiligo. Consequently, we explored which major protease(s) could be involved in the cleavage of E-cadherin and could lead to destabilization of melanocytes. Serum levels of both zymogen and active forms of MMP-9 were higher in patients with active vitiligo and psoriasis than in healthy controls (Figure 3, A and B), whereas MMP-3, MMP-7, and ADAM10 serum levels were similar in all groups (Supplemental Figure 6, A–C). MMP-9 levels were sig-nificantly higher in patients with vitiligo with active disease compared with those in healthy controls or in vitiligo patients with stable disease (Figure 3, A and B), and a positive correlation between total and active MMP-9 was observed in patients with vitiligo (Supplemental Figure 6D). Interestingly, MMP-9 levels correlated positively with soluble E-cadherin levels in the serum of patients with vitiligo as well as the body surface area involved (Figure 3, C and D, and Supplemental Figure 6, E and F). An increase in MMP-9 expression was observed at both the gene level and the protein level in active and stable vitiligo perilesional skin and lesional psoriasis skin, in comparison with healthy skin (Figure 3, E and F, and Supplemental Figure 6G). This was in contrast with MMP-3, MMP-7, and ADAM10 gene and protein expression, which remained lower and not significantly different among healthy control skin, vitiligo skin, and psoriasis skin, in comparison with strong MMP-9 upregulation (Supplemental Figure 6, H–J). We then compared the inflammatory transcriptome profile of the perilesional skin of patients with stable or active vitiligo using the nCounter inflammation panel (248 genes) to identify the genes that were the most differentially regulated. We found that the MMP9 gene was among the top 10 genes upregulated in active vitiligo skin (Figure 3G). The interactomic network of the upregulated transcripts showed MMP-9 to be at the core of the molecular signature identified, together with genes previously shown to be involved in depigmentation such as TNF and CXCL9 (Figure 3H). Last, TNF-α and IFN-γ strongly induced the expression and production of MMP-9 by epidermal cells, mainly by keratinocytes (Figure 3, I–K), whereas they had little or no effect on MMP-3, MMP-7, and ADAM10 expression (Supplemental Figure 7, A and B).

MMP-9 (also known as gelatinase B) belongs to the gelatinase subgroup of MMPs, which also includes MMP-2 (also known as gelatinase A). We therefore investigated whether MMP-2 was deregulated in our experimental setting. In contrast to MMP-9, levels of MMP-2 were decreased in the sera of patients with vitiligo, and a similar tendency was observed in psoriasis serum, although not significant (Supplemental Figure 8A). Nonetheless, MMP-2 serum levels did not correlate negatively with MMP-9 serum levels or the body surface area involved in patients with vitiligo (Supplemental Figure 8, B and C). In accordance with these findings, TNF-α and IFN-γ reduced MMP-2 levels in keratinocytes. MMP-2 expression was not detected in melanocytes (Supplemental Figure 8, D and E, and data not shown).

MMP-9 is involved in melanocyte detachment induced by type 1 cytokines in vitro and in vivo. We next explored the contribution of MMP-9 to melanocyte destabilization in RHPE and observed that active MMP-9 induced a dose-dependent increase in the proportion of suprabasal melanocytes, associated with an increase in soluble E-cadherin levels (Figure 4, A–C). Subsequent experiments using the gelatinase inhibitor SB-3CT or a selective inhibitor of MMP-9 (ab142180) investigated the effect of MMP-9 inhibition in RHPE treated with TNF-α and IFN-γ. We observed a modest and robust dose-dependent inhibition of melanocyte detach-ment induced by type 1 cytokines with both of the inhibitors tested (Figure 4, D and E). This effect was associated with a decrease in soluble E-cadherin levels (Figure 4F). To fully confirm this mechanism in vivo, both TNF-α and IFN-γ were injected intradermally into C57BL/6 WT mice every day for 6 days (Figure 4G). Owing to the low number of melanocytes in mouse skin, the mouse tail was used for injection because melanocytes are located in the basal layer of epidermis, thus reproducing human pigmentation. Consistent with human data, concomitant intradermal injection of IFN-γ and TNF-α induced a significant detachment of melanocytes associated with disruption of E-cadherin expression (Figure 4, H and I, and Supplemental Figure 9). In support of our results obtained in vitro, MMP-9 inhibition with SB-3CT was associated with a significant stabilization of epidermal melanocytes in the basal layer of the epidermis (Figure 4, H and I), thus providing further evidence of the involvement of MMP-9 in the process leading to melanocyte loss.

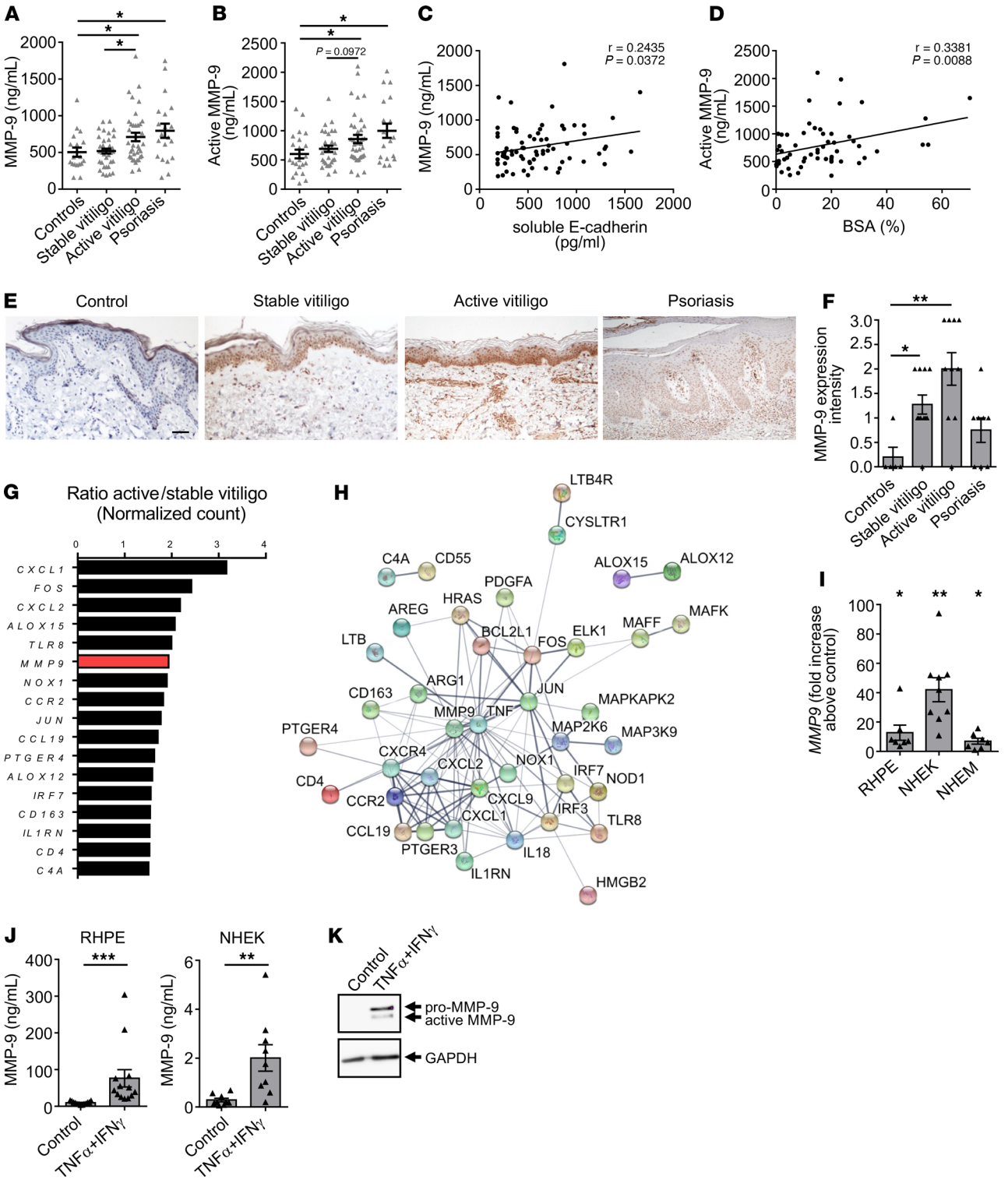

Figure 3. MMP-9 levels are increased in patients with vitiligo and correlate with soluble E-cadherin levels and surface of depigmentation. (**A**) ELISA levels of MMP-9 in the sera of healthy controls (n = 18), patients with stable (n = 37) or active (n = 37) vitiligo, and patients with psoriasis (n = 20). (**B**) Active MMP-9 levels in the sera of healthy controls (n = 22), patients with stable (n = 30) or active (n = 39) vitiligo, and patients with psoriasis (n = 19). (**C**) Spearman's rho correlation (2-tailed) between MMP-9 and soluble E-cadherin levels in the sera of patients with vitiligo (n = 73). (**D**) Spearman's rho correlation (2-tailed) between serum active MMP-9 and body surface area (BSA) involved in patients with vitiligo (n = 59). (**E**) Representative IHC staining of MMP-9 expression in healthy control skin, perilesional skin of stable and active vitiligo, and lesional psoriatic skin. Scale bar: 100μm. (**F**) Semiquantitative analysis of MMP-9 expression in skin from healthy controls (n = 5), perilesional skin of vitiligo patients with stable (n = 11) or active (n = 10) disease, and lesional psoriatic skin (n = 8). (**G** and **H**) Inflammatory transcriptomic profile of perilesional skin of patients with stable (n = 3) and active (n = 6) vitiligo was assessed using NanoString technology. (**G**) The most upregulated genes are shown. Results show the change in gene expression between the 2 groups. (**H**) Predicted protein-protein interaction networks for upregulated genes using STRING online tool.

The thickness of edges represents the strength of data support. The thicker the edge between 2 proteins, the more these proteins are linked based on the enrichment evidenced by STRING. (I and J) Reconstructed human pigmented epidermis (RHPE), NHEK, and NHEM were stimulated for 24 hours in the absence or presence of TNF-α and IFN-γ. (I) Real-time PCR analysis of *MMP9* gene expression in RHPE (n = 7), NHEK (n = 9), and NHEM (n = 7). Data are shown as fold increase above the control culture. *GAPDH* was used as a housekeeping gene. (J) Levels of MMP-9 in cell-free culture supernatants of RHPE (n = 13, left) and NHEK (n = 9, right). (K) Western blot analysis of MMP-9 expression in NHEK treated for 24 hours in the presence or absence of 20 ng/mL of TNF-α and IFN-γ. Data in A, B, F, I, and J show mean ± SEM. *P < 0.05, **P < 0.01, ***P < 0.001; calculated with Kruskal-Wallis (A, B, and F) or Wilcoxon tests (I and J).

Inhibition of JAK signaling stabilizes melanocytes in the basal layer of the epidermis by MMP-9 reduction. To further decipher the mechanism involved in melanocyte destabilization, we studied the effect of JAK sig-naling using tofacitinib (a JAK1/3 inhibitor) or ruxolitinib (a JAK1/2 inhibitor) in our in vitro and in vivo models of melanocyte detachment induced by TNF-α and IFN-γ. Both JAK inhibitors led to significant melanocyte stabilization in RHPE treated with TNF-α and IFN-γ (Figure 5, A and B), associated with a decrease in levels of soluble E-cadherin and active MMP-9 (Figure 5, C and D). A decrease in MMP9 levels was also observed in vitro on vitiligo perilesional epidermis explants after tofacitinib treatment (Figure 5E). Inhibition of JAK signaling also prevented melanocyte detachment induced by type 1 cytokines in vivo (Figure 5, F and G), and no significant difference was noted between the 2 inhibitors tested in our models.

Discussion

Our findings shed light on a so far unknown mechanism regarding the interplay between the inflammatory response and melanocyte loss in vitiligo. We demonstrate that destabilization of melanocytes from the basal layer of the epidermis is an important event leading to their loss. This destabilization results from alteration of membrane E-cadherin in response, at least in part, to the upregulated production of active MMP-9 by epidermal cells, especially keratinocytes, induced by the type 1 cytokines IFN-γ and TNF-α, which are 2 proinflammatory cytokines involved in vitiligo. This phenomenon could be reproduced by administering active MMP-9 or prevented by using MMP-9 inhibitors or by inhibiting the JAK/STAT signaling pathway with JAK inhibitors (Figure 6).

Importantly, the suprabasal localization of melanocytes within the epidermis is not restricted to vitiligo, and the mechanism hereby identified could occur in the hypopigmentation associated with other causes of chronic skin inflammation, as in psoriasis. Indeed, we recently reported that hypopigmentation could occur in 10% of patients with psoriasis and was observed in areas previously affected by the disease (37). However, in contrast to vitiligo, complete and durable depigmentation was not observed in psoriasis, perhaps due to (a) the proliferative capacity of melanocytes, which is greater in lesional psoriatic skin than in vitiligo perilesional skin, and (b) to apoptosis of suprabasal melanocytes in vitili-go, as previously reported (26), which could involve the recently identified innate lymphocyte-induced CXCR3B-mediated apoptosis (38).

Another explanation could be that melanocytes in patients with vitiligo have intrinsic abnormalities that cause a regenerative deficiency (2, 3). Indeed, the activation, maturation, proliferation, and recruitment of melanocyte precursors in vitiligo skin are defective (39), explaining the persistence of white patches. This contrasts with lesional psoriatic skin, which harbors a high proportion of proliferating melanocytes, explaining not only the absence of complete depigmentation in patients despite melanocyte detachment from the basal layer of the epidermis, but also the fact that depigmented lesions are able to recover rapidly under therapies. This is consistent with previous reports showing an increased number of melanocytes both in psoriasis lesions and in resolved psoriasis skin (40, 41).

Our data suggest that the death of melanocytes, especially in patients with vitiligo, could occur after their detachment and relocalization to the outer layers of the epidermis (melanocytorrhagy), as previously observed (26). Vitiligo is characterized by clinically undetectable and pathologically mild inflammation with infiltration of melanocyte-specific resident memory CD8 T cells producing elevated levels of proinflammatory cytokines, whereas the production of cytotoxic markers was similar to healthy skin and lesional psoriasis skin (7). Interestingly, it was recently demonstrated that a melano-cyte antigen can trigger autoimmunity in psoriasis with skin infiltration of epidermal melanocyte-specific CD8 T cells producing proinflammatory cytokines involved in the development of psoriasis, such as IL-17 and IFN-γ (42). However, although granules containing granzyme B were identified in a CD8 T cell subset from psoriasis skin, the authors failed to detect any signs of cell death in melanocytes. In view of our findings, we hypothesize that IFN-γ and TNF-α, produced by resident memory T cells in vitiligo skin, contribute to melanocyte destabilization. Our observations contrast with what may be observed in other inflammatory skin disorders, such as the group of lichenoid dermatitis associated with cutaneous lupus disease and lichen planus. These diseases are characterized by strong immune infiltration of the basal layer, leading to the destruction of epidermal cells such as melanocytes, the release of melanin in the dermis (incontinence), and to definitive cicatricial pigmentary changes (43).

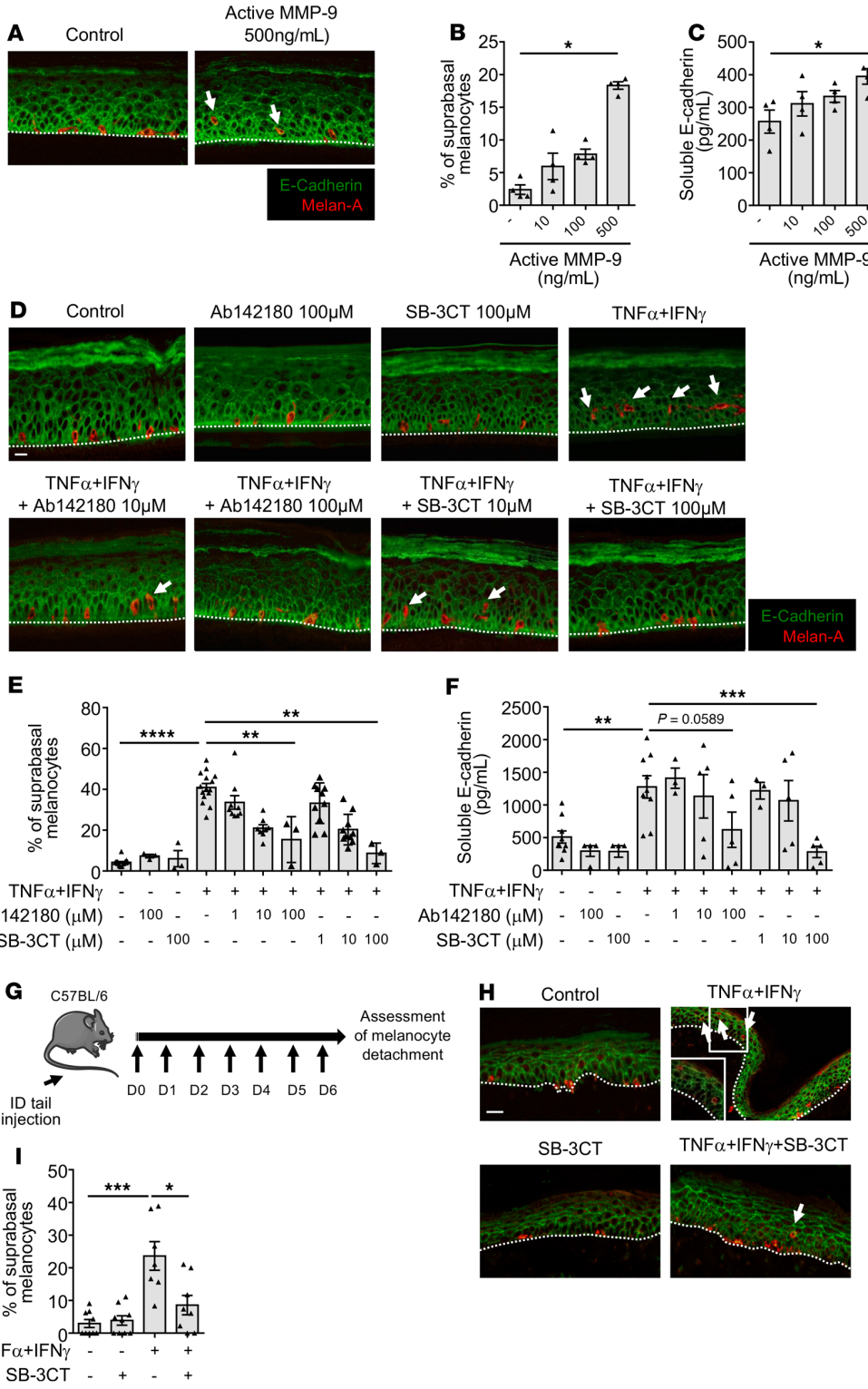

Figure 4. MMP-9 inhibition allows melanocyte stabiliza-tion both in vitro and in vivo. (**A**–**C**) Reconstructed human pigmented epidermis (RHPE) were treated for 24 hours in the presence or absence of increas-ing concentrations of active MMP-9. (**A**) Representative immunofluorescence staining of Melan-A (red) and E-cad-herin (green). Dashed lines represent the dermoepidermal layer. Arrows show suprabasal melanocytes in the different conditions. Scale bar: 20 µm. (**B**) Proportion of suprabasal melanocytes in the different conditions. (**C**) Assessment by ELISA of soluble E-cadherin levels in cell-free supernatants.(**D**–**F**) RHPE were treated for 24 hours in the presence or absence of 10 ng/mL of TNF-α and IFN-γ and/or 1, 10 or 100 µM of MMP-9 inhibitors Ab142180 or SB-3CT. (**D**) Repre-sentative immunofluorescence staining of Melan-A (red) and E-cadherin (green). Dashed lines represent the dermoepi-dermal layer. Arrows show suprabasal melanocytes in the different conditions. Scale bar: 20 µm. (**E**) Proportion of suprabasal melanocytes in the different culture conditions. (F)) Assessment by ELI A of soluble E-cadherin levels in cell-free supernatants. (G–I) The base of C57BL/6 mouse tail was treated daily for 6 days with intradermal injections of saline buffer (control), or the combination of 1 µg of TNF-α and IFN-γ and/or 1.25 mg/mL of SB-3CT. (G) In vivo schema of C57BL/6 mice treatment. (H) Representative immu-nofluorescence analysis of Melan-A (red) and E-cadherin (green) staining in the different groups. Dashed lines represent the dermoepidermal layer. Arrows show suprabasal mela-nocytes. Scale bars: 20 µm. (I) Proportion of suprabasal melanocytes was assessed in the different groups (n = 7–9). Data in B, C, E, F, and I show mean ± SEM. *P < 0.05, **P < 0.01, ***P < 0.001; ****P < 0.0001, calculated with 2-tailed Mann-Whitney test.

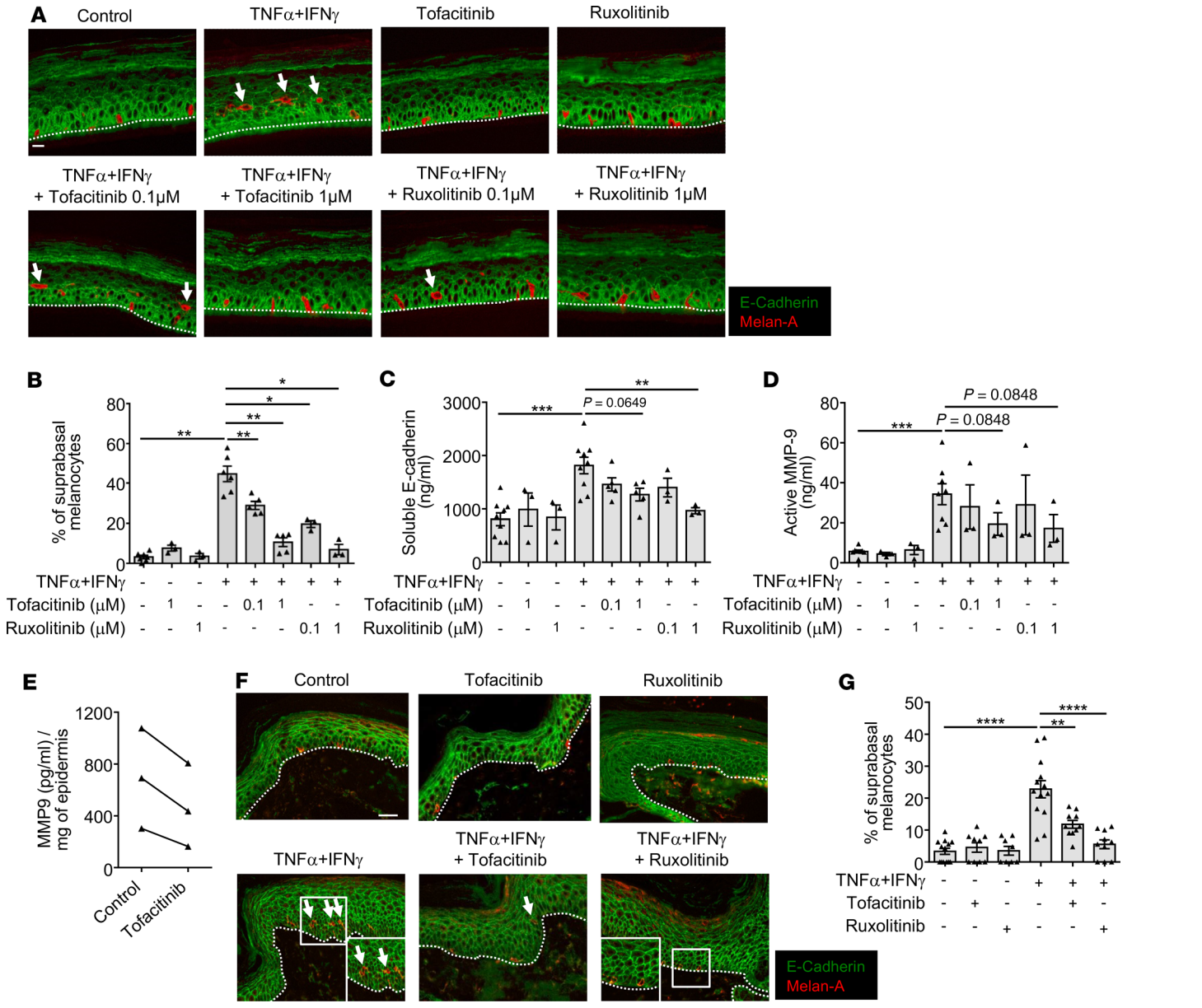

Figure 5. Inhibition of JAK prevents type 1 cytokine-mediated melanocyte detachment both in vitro and in vivo. (**A**–**D**) Reconstructed human pigmented epidermis (RHPE) were treated for 24 hours in the presence or absence of 10 ng/mL of TNF-α and IFN-γ and/or 0.1 or 1 μM of tofacitinib or ruxolitinib. (**A**) Rep-resentative immunofluorescence staining of Melan-A (red) and E-cadherin (green). Dashed lines represent the dermoepidermal layer. Arrows show suprabasal melanocytes in the different conditions. Scale bar: 20 μm. (**B**) Proportion of suprabasal melanocytes in the different culture conditions. (**C** and **D**) Assessment by ELISA of (**C**) soluble E-cadherin or (**D**) active MMP-9 levels in cell-free supernatants. (**E**) Vitiligo perilesional epidermis were treated for 24 hours in the presence or absence of 1μM of tofacitinib. MMP-9 levels were assessed by ELISA in cell-free supernatants ($n = 3$). (**F** and **G**) C57BL/6 mouse tails were treated by intradermal injection of saline solution (control), 1 μg TNF-α and IFN-γ, and/or 1 mM of tofacitinib or ruxolitinib, according to the same protocol described in Figure 4F. (**F**) Representative immunofluorescence analysis of Melan-A (red) and E-cadherin (green) staining in the different groups. Dashed lines represent the dermoepidermal layer. Arrows show suprabasal melanocytes. Scale bars: 20 μm. (**G**) Proportion of suprabasal melanocytes was assessed in the different groups ($n = 6$–10). Data in **B**–**D** and **G** show mean ± SEM. *$P < 0.05$, **$P < 0.01$, ***$P < 0.001$; ****$P < 0.0001$, calculated with 2-tailed Mann-Whitney test.

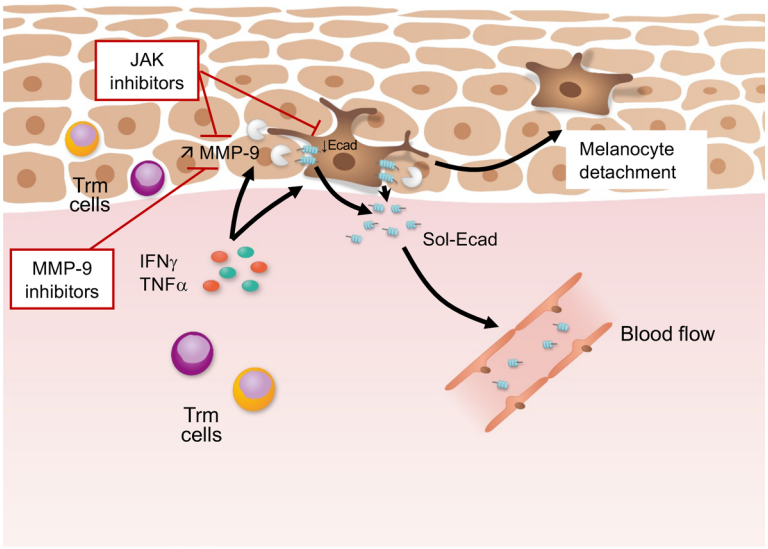

Figure 6. Putative model of primary event leading to loss of melanocytes in depigmenting disorders. Type 1 cytokines TNF-α and IFN-γ produced by activated Trm cells induce an E-cadherin defect in melanocytes. TNF-α and IFN-γ induce the production of MMP-9 by epidermal cells, especially keratinocytes, that cleave E-cadherin (Ecad) to release its soluble form. E-cadherin cleavage leads to melanocyte destabilization. This effect is inhibited in the presence of MMP-9 or JAK inhibitors.

Our data reveal a previously unknown role of MMP-9 during depigmentation and highlight its prominent role in inducing melanocyte destabilization by the shedding of E-cadherin and the release of its soluble form. Besides type 1 cytokines, additional cytokines upregulated in the blood and/or skin of patients with vitiligo and known to increase MMP-9 expression could also be involved in its upregulation, including IL-1β, IL-17, or IL-6 (30, 31, 44). In line with a study suggesting the low production of MMP-9 by melanocytes in patients with vitiligo (45), we found that keratinocytes were the main epidermal source of MMP-9. In contrast, another gelatinase, MMP-2, was found to be decreased in the sera of patients with vitiligo, and its production was found to be downregulated by IFN-γ and TNF-α. MMP-2 is known to be involved in the migration of melanocyte precursors for their optimal epidermal replenishment (46). MMP-2 reduction, together with the increase in MMP-9 production, could therefore effect simultaneously the stabilization of epidermal melanocytes and their replenishment from the melanocyte precursor reservoir, thus leading to durable depigmentation in vitiligo. However, although we could not identify any increased expression of some other proteases (e.g., MMP-3, MMP-7, ADAM10) known to play a role in E-cadherin cleavage, we cannot rule out the possibility that other proteases not evaluated in this study are involved in this process. This is supported by the fact that the treatment of RHPE with active MMP-9 induced a significant but lower melanocyte detachment than that observed in response to IFN-γ and TNF-α. Additionally, it would be relevant in psoriasis to test the role of Th17-related cytokines alone or in combination with Th1-related cytokines in this phenomenon. We now need to focus on 2 major goals in vitiligo therapy: first, dampening the activation of the immune response responsible for the loss of melanocytes and the maintenance of depigmentation; and second, maintaining melanocytes in the basal layer and promoting their regeneration from melanocyte precursors. Like other MMPs, MMP-9 is known to be upregulated in autoimmune and inflammatory disorders and to play a role in modulating the innate and adaptive immune response, the production of chemokine ligands and cytokine activity (47). Therefore, in vitiligo and other chronic depigmenting disor-ders associated with inflammation, the inhibition of MMP-9 activity with topical or systemic agents could both dampen the immune response and help to stabilize melanocytes in the basal layer of the epidermis. Moreover, our study provides evidence that targeted therapies such as topical or systemic JAK inhibitors, which have shown promising results in vitiligo (48–51), could inhibit the type II IFN response, thereby maintaining melanocytes in the basal layer of the epidermis. Hence, the association of JAK inhibitors together with MMP-9 inhibitors could be a way to lower the dose of each component for either systemic or topical applications, ideally in combination with a therapy that stimulates melanocyte regeneration such as phototherapy. Although our study provides new insights into the targeting of MMP-9 in vitiligo, it is now critical to confirm this strategy in preclinical models of vitiligo. Mouse models of skin depigmentation after infiltration of melanocyte-specific CD8 T cells are available (52) and could be used to fully validate a strategy to inhibit melanocyte detachment through targeting of MMP-9. Showing that the use of a MMP-9 inhibitor alone or in combination with immunomodulating agents could either prevent depigmentation or induce repigmentation would be of great interest before going to clinical trials. We now need to set the therapeutic objective of stabilizing melanocytes in the basal layer of the epidermis with specific therapies able to restore the expression of membrane E-cadherin or to inhibit its cleavage.

Methods

Subjects, skin, and serum samples. Human peripheral blood and skin punch biopsy samples were obtained from patients with vitiligo and psoriasis from the Department of Dermatology in Bordeaux University Hospital. None of the patients included in this study had received any treatments/immunosuppressive therapies during the 6 months preceding inclusion. The clinical characteristics of patients are presented in Supplemental Tables 1 and 2. Patients with vitiligo were classified according to the Vitiligo European Task Force (VETF) scoring system, as described previously (53), notably for disease activity. Briefly, they were classified using Wood's lamp examinations, as previously reported (54, 55). Patients with a total spreading score greater than or equal to 3, according to the VETF scoring system and/or the presence of hypomelanotic lesions with poorly defined borders and/or confetti-like lesions, were considered active, whereas those with a total spreading score less than or equal to 1 and/or the absence of new lesions over the past 12 months were considered stable. Skin biopsies (4-mm diameter) were obtained from the perile-sional area. Lesional psoriatic skin biopsies were obtained as a control of skin inflammatory disorder. Paraffin-embedded skin sections from patients with cutaneous lupus and toxic epidermal necrolysis were obtained from the Department of Pathology at Bordeaux University Hospital. Unaffected control skin was obtained as discarded human tissue from cutaneous plastic surgery (Bordeaux University Hospital). Blood from unaffected subjects was obtained from volunteers exempt of autoimmune or inflammatory disorders.

Cell cultures and cytokine treatment. Primary human melanocytes were isolated from healthy children's fore-skin as previously described (56), maintained in melanocyte growth medium, and supplemented with basic recombinant human fibroblast growth factor (1 ng/mL), hydrocortisone (0.5 μg/mL), bovine pituitary extract (4 μg/mL), recombinant human insulin (5 μg/mL) (all from Promo Cell), and penicillin (100 U/mL) and streptomycin (100 μg/mL) (Eurobio). Primary human keratinocytes were obtained from surgical samples of healthy breast skin as previously described (57). Cells were cultivated in keratinocyte serum-free medium (Life Technologies) and supplemented with bovine pituitary extract (25 μg/mL), epidermal growth factor (0.25 ng/mL) (Life Technologies), penicillin (100 U/mL) (Eurobio), and streptomycin (100 μg/mL) (Eurobio). Cells were maintained in a humidified atmosphere 5% CO_2 at 37°C and starved in growth factor–free medium before stimulation with indicated concentrations of TNF-α and IFN-γ (R&D Systems), alone or in combina-tion. Cell-free supernatants were harvested for ELISA and remaining cells were lysed for RNA quantification or Western blot analysis. In vitro RHPE containing both melanocytes and keratinocytes were generated from surgical samples of pediatric foreskins on polycarbonate culture inserts (Bioalternatives Laboratories). RHPE were cultured at the air–liquid interphase for 10 days in a humidified atmosphere 5% CO_2 at 37°C and then treated for 24 hours with or without TNF-α and IFN-γ (10 ng/mL), alone or in combination (R&D Systems). When appropriate, indicated concentrations of active MMP-9 (MilliporeSigma), SB-3CT, selective Ab142180 MMP-9 inhibitor (Abcam), tofacitinib (MilliporeSigma), or ruxolitinib (Stemcell) were added. Perilesional skin explants were incubated 3 hours at 37°C with trypsin-EDTA to isolate the epidermis. Epidermal sheets were then treated 24 hours with or without tofacitinib (1 μM). Cell-free supernatants were harvested for ELISA.

Animal studies. C57BL/6j WT mice were purchased from Charles River Laboratories and were housed in an animal facility at the University of Bordeaux under conventional conditions with constant tempera-ture and humidity. Mice were injected intradermally daily (from day 0 to day 6) with PBS and/or TNF-α (1 μg) and IFN-γ (PeproTech) and/or tofacitinib (1 mM) (MilliporeSigma), ruxolitinib (1 mM), or SB-3CT (1.25 mg/mL) (Abcam), in the base of the tail. On day 7, mice were sacrificed, the tail was fixed in forma-lin, and paraffin-embedded sections were prepared to perform immunofluorescence studies.

Cell proliferation analysis. Cell proliferation was measured using the premix WST-1 cell proliferation assay system (Takara Bio). Cells were treated with increasing concentrations of TNF-α and/or IFN-γ (ranging from 0.2 to 200 ng/mL) for 24, 48, and 72 hours at 37°C. Ten microliters of WST-1 were added 4 hours before measurement of the absorbance at 450 nm and 650 nm to determine proliferation and back-ground absorbance, respectively (Multiskan FC Microplate Reader, Thermo Fisher Scientific).

NanoString. The nCounter technology was performed by the "Groupe de Recherche en Immunol-ogie Clinique" (GRIC) at Bordeaux University Hospital. RNA was extracted from FFPE skin sections of patients with stable (n = 3) or active (n = 6) vitiligo using the High Pure FFPET RNA Isolation Kit (Roche). RNA purity and concentrations were determined using NanoDrop and Bioanalyzer 2100 (Agi-lent RNA 6000 Nanokit). Samples were processed with Nanostring CodeSet technology and the NanoS-tring nCounter Human Inflammation panel v2 mRNA Expression Assay (NanoString Technologies). Results were analyzed using the nSolver Analysis Software 4.0 (NanoString). The software STRING (Search Tool for the Retrieval of Interacting Genes, v.10.5 web server, http://strindb.org/, under a "Creative Commons BY 4.0" license), with Homo sapiens as the reference organism, was used to generate an association network of potentially interacting proteins, with a minimum required interaction score of 0.4. The network was built following the automatic enrichment in STRING, based on the information provided by several databases such as KEGG, Ensembl, and BioCyc.

Quantitative real-time PCR analysis. Total RNA was isolated from primary human epidermal keratinocytes or melanocytes using NucleoSpin RNA and Nucleospin RNA XS kits (Macherey-Nagel), respectively. RNA from tissue samples and RHPE were extracted using TRIzol reagent (Invitrogen Life Technologies). RNA (200 ng to 1 μg) was then retrotranscribed with 1X first-strand buffer, random primers (0.25 μg/μl), dNTP (0.02 M), dithiothreitol (0.03 μM), and SuperScript II Reverse Transcrip-tase (100 U) (Invitrogen), according to the manufacturer's instructions. Quantitative real-time PCR was carried using the Brilliant III Ultra-Fast SYBR Green QPCR Master Mix kit (Agilent Technologies), according to the manufacturer's instructions, together with gene-specific primers for *ADAM10*, *CCN3*, *CDH1*, *CTNNB1*, *DDR1*, *MMP2*, *MMP3*, *MMP7*, and *MMP9*. *GAPDH* was used as a housekeeping gene. After an initial step at 95C° for 3 minutes, cDNA was amplified for 40 cycles (15 seconds at 95°C, 22 seconds at 60 or 64°C) in a MX3000P Stratagene thermocycler (Agilent Technologies). Human primer sequences are as follows: *ADAM10,* 5′-CCTGAAGTGGAGCGAGAGGG-3′ (sense) and 5′-CATACT-GACCTCCCATCCCCG-3′ (antisense); *CCN3*, 5′-CGGCTGCTCATGCTGTCTGG-3′ (sense) and 5′-TTATCTCCCTCTACCGCCGTGC-3′ (antisense); *CDH1,* 5′-ATCCTCCGATCTTCAATCCCAC-CAC-3′ (sense) and 5′-GTACCACATTCGTCACTGCTACGTG-3′ (antisense); *CTNNB1,* 5′-GGCCT-GTAGAGTTGCTGGAG-3′ (sense) and 5′-ACAAGCAAGGCTAGGGTTTG-3′; *DDR1*, 5′-GGGAA-GAGCGATGAGAGGTGT-3′ (sense) and 5′-TAGCTCCTGATCCCTCGGGC-3′ (antisense); *MMP2*, 5′-CGACCACAGCCAACTACGAT-3′ (sense) and 5′-GTCAGGAGAGGCCCCATAGA-3′ (anti-sense); *MMP3*, 5′-GCCAGGCTTTCCCAAGCAAAT-3′ (sense) and 5′-GTCACAGCACAGGCAG-GAGAAA-3′ (antisense); *MMP7*, 5′-GGATACTTCCACAGGTCCCAC-3′ (sense) and 5′-ACGG-GACTGGAAGCCCTTTT-3′ (antisense); *MMP9*, 5′-GTACTCGACCTGTACCAGCG-3′ (sense) and 5′-TTCAGGGCGAGGACCATAGA-3′ (antisense); and *GAPDH*, 5′-GGCTCTCCAGAACATCATC-CCTGC-3′ (sense) and 5′-GGGTGTCGCTGTTGAAGTCAGAGG-3′ (antisense). The $2^{-\Delta\Delta CT}$ method was used to determine relative gene expression level after normalization to expression of *GAPDH*.

Immunohistochemistry/immunofluorescence studies. We prepared 4-μm sections from FFPE skin biop-sies. Sections were deparaffinized and subjected to a heat-induced epitope retrieval step. Slides were rinsed in cool running water and washed in Tris-buffered saline (pH 7.4) before incubation overnight at 4°C with relevant primary antibodies. Primary antibodies used for immunofluorescence experiments were as follows. For human skin tissues: mouse monoclonal anti–Melan-A antibody (A103, M7196, Dako, 1/100); mouse monoclonal anti-MITF antibody (D5, M3621, Dako, 1/100); rabbit polyclonal anti–E-cadherin (ab15148, Abcam, 1/100); rabbit polyclonal anti–type VII collagen (ab93350; Abcam, 1/100); rabbit monoclonal anti-Ki67 (SP6, ab16667, Abcam, 1/100); rabbit polyclonal cleaved–caspase-3 (Asp175, Cell Signaling, 1/100); and mouse monoclonal anti–LAMP-1/CD107a antibody (5E7, NBP2-52721, Novus Bio, 1/50). For mouse skin tissues: mouse monoclonal anti–E-cadherin (M168, ab76055, Abcam, 1/200) and rabbit monoclonal anti–Melan-A (A19-P, NovusBio, 1/2000). Secondary antibodies used were Alexa 555 goat anti–mouse IgG (A21422, Life technologies, 1/1000) and Alexa 488 goat anti–rabbit IgG (H+L) (ab150077, Abcam, 1/200).

After subsequent washing, the sections were mounted with Prolong Gold antifade reagent with DAPI (Thermo Fisher Scientific). Appropriate isotype-matched controls were included. TUNEL assay was performed using a commercially available kit (In Situ Cell Death Detection, Roche) according to the manufacturer's protocol. For IHC, slides were incubated overnight at 4°C with relevant primary anti-bodies: rabbit polyclonal anti–MMP-3 antibody (NB100-91878, Novus Bio, 1/50); mouse monoclonal anti–MMP-7 antibody (MM0022-4C21, NB110-60988, Novus Bio, 1/200); rabbit polyclonal anti–MMP-9 antibody (NB600-1217, Novus Bio, 1/2000); and rabbit polyclonal anti–ADAM10 antibody - Cyto-plasmic domain (ab39177, Abcam, 1/2000). Secondary labeling was performed using the LSAB2 kit (DAKO). Two individuals independently analyzed the stained slides in a blinded manner. Expression of MMP-3, MMP-7, MMP-9, and ADAM10 was scored using a semiquantitative method (0, no expression; 1, weak expression; 2, fair expression; 3, strong expression). Images were acquired using an epifluores-cence microscope (Leica) or LSM 510 META confocal laser-scanning microscope (Carl Zeiss).

Western blot analysis. To perform immunoblotting, keratinocytes were lysed in a cell lysis buffer (Cell Signaling) and supplemented with phenylmethylsulfonyl fluoride (1 mM) (MilliporeSigma) according to the manufacturer's instructions. Protein concentrations were measured using a BCA Protein Assay Kit (Pierce). Protein lysates (15 μg) were separated by 10% SDS-PAGE gel electropho-resis and transferred to a PVDF membrane (GE Healthcare). MMP-9 and GAPDH were detected using rabbit anti–MMP-9 antibody (E11, sc-393859, Santa-Cruz, 1/250) and rabbit anti–GAPDH antibody (14C10, 2118, Cell Signaling, 1/1000), respectively, and peroxidase–conjugated goat anti–rabbit antibody (7074, Cell Signaling, 1/2000) according to the manufacturer's instructions. Detection was carried out using the ECL detection system (Bio-Rad) and a chemiluminescent image analyzer (LAS-3000, Fujifilm).

ELISA. Concentrations of soluble E-cadherin, MMP-2, MMP-7, MMP-3, MMP-9 (all from R&D systems), and ADAM10 (Elab Science Biotechnology) in the sera of patients and/or cell-free culture supernatants were measured according to the manufacturers' instructions. Levels of the active form of MMP-9 were quantified using the Fluorokine Human Active MMP-9 kit (R&D Systems) according to the manufacturer's instructions, and 4-aminophenylmercuric acetate was added to samples.

Statistics. All statistical analyses were performed using GraphPad Prism 6 software. Data are presented as mean ± SEM unless otherwise indicated. Spearman's rank correlations were used for all correlation coefficients. Nonparametric (Mann-Whitney or Wilcoxon tests) 2-tailed paired and unpaired *t* tests were used to compare 2 groups at 95% confidence interval. To determine statistical differences among controls, vitiligo, and psoriasis groups, the normal distribution and the homogeneity of variances were first tested using the Shapiro-Wilk and Bartlett tests, respectively. When the variables fit with normal distribution and were equal, the 1-way ANOVA was used. In other cases, a Kruskal-Wallis test was performed. Differences were considered statistically significant when *P* values were less than or equal to 0.05.

Study approval. All studies involving human tissues were approved by the Ethics Committee and the Commission Nationale de l'Informatique et des Libertés (no. 1545937). All subjects provided written informed consent for inclusion in this study. Experimental procedures on animals were conducted in compliance with the guidelines of the ethical committee of the University of Bordeaux and approved by the national French animal welfare laws, guidelines, and policies (APAFIS 7406).

Author contributions

JS and KB conceived and supervised the study. NB, CM, FM, FXB, JS, and KB designed the experiments. NB, ASD, CM, JR, CB, JG, CD, CJ, DT, and FL performed the experiments. NB, CM, JS, and KB ana-lyzed data. ASD, KE, AT, and JS contributed to clinical samples. NB, CM, JS, and KB prepared the figures. JS and KB wrote the manuscript. All authors revised the manuscript.

Acknowledgments

We thank I. Pellegrin, A Tarricone, A. Bru, and C. Larmonier (Groupe de Recherche en Immunolo-gie Clinique, Bordeaux University Hospital Center) for their contribution to transcriptome analysis with the Nanostring technology, and R. Cooke for copyediting. This work was supported by the ATIP-AVENIR, Agence nationale de la recherche Young Researchers (JCJC), and "Société Française de Dermatologie" grants.

Address correspondence to: Katia Boniface, INSERM U1035, BMGIC – Immunodermatology team, Uni-versity of Bordeaux, 146 rue Léo Saignat, Bâtiment TP zone sud, 4ème étage, 33076 Bordeaux Cedex, France. Phone: 33.0.5.57.57.13.73; Email: katia.boniface@u-bordeaux.fr.

1. Vachiramon V, Thadanipon K. Postinflammatory hypopigmentation. *Clin Exp Dermatol*. 2011;36(7):708–714.
2. Picardo M, et al. Vitiligo. *Nat Rev Dis Primers*. 2015;1:15011.
3. Boniface K, Seneschal J, Picardo M, Taïeb A. Vitiligo: focus on clinical aspects, immunopathogenesis, and therapy. *Clin Rev Allergy Immunol*. 2018;54(1):52–67.
4. Boniface K, Taïeb A, Seneschal J. New insights into immune mechanisms of vitiligo. *G Ital Dermatol Venereol*. 2016;151(1):44–54.
5. Camara-Lemarroy CR, Salas-Alanis JC. The role of tumor necrosis factor- α in the pathogenesis of vitiligo. *Am J Clin Dermatol*. 2013;14(5):343–350.
6. Englaro W, et al. Tumor necrosis factor α-mediated inhibition of melanogenesis is dependent on nuclear factor κ B activation. *Oncogene*. 1999;18(8):1553–1559.
7. Boniface K, et al. Vitiligo skin is imprinted with resident memory CD8 T cells expressing CXCR3. *J Invest Dermatol*. 2018;138(2):355–364.
8. Cheuk S, et al. CD49a expression defines tissue-resident $CD8^+$ T cells poised for cytotoxic function in human skin. *Immunity*. 2017;46(2):287–300.
9. Richmond JM, et al. Antibody blockade of IL-15 signaling has the potential to durably reverse vitiligo. *Sci Transl Med*. 2018;10(450):eaam7710.
10. Wańkowicz-Kalińska A, et al. Immunopolarization of $CD4^+$ and $CD8^+$ T cells to Type-1-like is associated with melanocyte loss in human vitiligo. *Lab Invest*. 2003;83(5):683–695.
11. Harris JE, Harris TH, Weninger W , Wherry EJ, Hunter CA, Turka LA. A mouse model of vitiligo with focused epidermal depigmentation requires IFN-γ for autoreactive $CD8^+$ T-cell accumulation in the skin. *J Invest Dermatol*. 2012;132(7):1869–1876.
12. Rashighi M, et al. CXCL10 is critical for the progression and maintenance of depigmentation in a mouse model of vitiligo. *Sci Transl Med*. 2014;6(223):223ra23.
13. Gregg RK, Nichols L, Chen Y, Lu B, Engelhard VH. Mechanisms of spatial and temporal development of autoimmune vitiligo in tyrosinase-specific TCR transgenic mice. *J Immunol*. 2010;184(4):1909–1917.
14. Yang L, et al. Interferon- γ inhibits melanogenesis and induces apoptosis in melanocytes: a pivotal role of $CD8^+$ cytotoxic T lym-phocytes in vitiligo. *Acta Derm Venereol*. 2015;95(6):664–670.
15. Swope VB, Abdel-Malek Z, Kassem LM, Nordlund JJ. Interleukins 1 α and 6 and tumor necrosis factor-α are paracrine inhibi-tors of human melanocyte proliferation and melanogenesis. *J Invest Dermatol*. 1991;96(2):180–185.
16. Natarajan VT, et al. IFN-γ signaling maintains skin pigmentation homeostasis through regulation of melanosome maturation. *Proc Natl Acad Sci U S* A. 2014;111(6):2301–2306.
17. van den Boorn JG, et al. Autoimmune destruction of skin melanocytes by perilesional T cells from vitiligo patients. *J Invest Der-matol*. 2009;129(9):2220–2232.
18. Sandoval-Cruz M, et al. Immunopathogenesis of vitiligo. *Autoimmun Rev*. 2011;10(12):762–765.
19. Riding RL, Harris JE. The role of memory $CD8^+$ T cells in vitiligo. *J Immunol*. 2019;203(1):11–19.
20. van den Wijngaard R, Wankowicz-Kalinska A, Le Poole C, Tigges B, Westerhof W, Das P. Local immune response in skin of generalized vitiligo patients. Destruction of melanocytes is associated with the prominent presence of CLA^+ T cells at the per-ilesional site. *Lab Invest*. 2000;80(8):1299–1309.
21. Wu J, Zhou M, Wan Y, Xu A. $CD8^+$ T cells from vitiligo perilesional margins induce autologous melanocyte apoptosis. *Mol Med Rep*. 2013;7(1):237–241.
22. Gauthier Y, Cario Andre M, Taïeb A. A critical appraisal of vitiligo etiologic theories. Is melanocyte loss a melanocytorrhagy? *Pigment Cell Res*. 2003;16(4):322–332.
23. Le Poole IC, van den Wijngaard RM, Westerhof W, Das PK. Tenascin is overexpressed in vitiligo lesional skin and inhibits melanocyte adhesion. *Br J Dermatol*. 1997;137(2):171–178.
24. Gumbiner BM. Regulation of cadherin-mediated adhesion in morphogenesis. *Nat Rev Mol Cell Biol*. 2005;6(8):622–634.
25. Tang A, Eller MS, Hara M, Yaar M, Hirohashi S, Gilchrest BA. E-cadherin is the major mediator of human melanocyte adhesion to keratinocytes in vitro. *J Cell Sci*. 1994;107(pt 4):983–992.
26. Wagner RY, et al. Altered E-cadherin levels and distribution in melanocytes precede clinical manifestations of vitiligo. *J Invest Dermatol*. 2015;135(7):1810–1819.
27. Delmas V, Larue L. Molecular and cellular basis of depigmentation in vitiligo patients.*Exp Dermatol*. 2019;28(6):662–666.
28. Khokha R, Murthy A, Weiss A. Metalloproteinases and their natural inhibitors in inflammation and immunity. *Nat Rev Immu-nol*. 2013;13(9):649–665.
29. David JM, Rajasekaran AK. Dishonorable discharge: the oncogenic roles of cleaved E-cadherin fragments.*Cancer Res*. 2012;72(12):2917–2923.
30. Harris JE, Fernandez-Vilaseca M, Elkington PT , Horncastle DE, Graeber MB, Friedland JS. IFNγ synergizes with IL-1β to up-regulate MMP-9 secretion in a cellular model of central nervous system tuberculosis. *FASEB J*. 2007;21(2):356–365.
31. Zhou L, et al. Tumor necrosis factor- α induced expression of matrix metalloproteinase-9 through p21-activated kinase-1. *BMC Immunol*. 2009;10:15.
32. Ram M, Sherer Y, Shoenfeld Y. Matrix metalloproteinase-9 and autoimmune diseases. *J Clin Immunol*. 2006;26(4):299–307.
33. Hu J, Van den Steen PE, Sang QX, Opdenakker G. Matrix metalloproteinase inhibitors as therapy for inflammatory and vascu-lar diseases. *Nat Rev Drug Discov*. 2007;6(6):480–498.
34. Benson HL, et al. Endogenous matrix metalloproteinases 2 and 9 regulate activation of $CD4^+$ and $CD8^+$ T cells. *Am J Respir Cell Mol Biol*. 2011;44(5):700–708.
35. Hawkes JE, Chan TC, Krueger JG. Psoriasis pathogenesis and the development of novel targeted immune therapies.*J Allergy Clin Immunol*. 2017;140(3):645–653.
36. Chen HR, et al. DDR1 promotes E-cadherin stability via inhibition of integrin- β1-Src activation-mediated E-cadherin endocyto-sis. *Sci Rep*. 2016;6:36336.
37. Amico S, et al. Characteristics of postinflammatory hyper- and hypopigmentation in patients with psoriasis: A survey study [published ahead of print February 14, 2020]. *J Am Acad Dermatol*. https://doi.org/10.1016/j.jaad.2020.02.025.
38. Tulic MK, et al. Innate lymphocyte-induced CXCR3B-mediated melanocyte apoptosis is a potential initiator of T-cell autoreactivity in vitiligo. Nat Commun. 2019;10(1):2178.
39. Birlea SA, Costin GE, Roop DR, Norris DA. Trends in regenerative medicine: repigmentation in vitiligo through melanocyte stem cell mobilization. Med Res Rev. 2017;37(4):907–935.
40. Wang CQF, et al. IL-17 and TNF synergistically modulate cytokine expression while suppressing melanogenesis: potential rele-vance to psoriasis. J Invest Dermatol. 2013;133(12):2741–2752.
41. Abdel-Naser MB, Liakou AI, Elewa R, Hippe S, Knolle J, Zouboulis CC. Increased activity and number of epidermal melano-cytes in lesional psoriatic skin. Dermatology (Basel). 2016;232(4):425–430.
42. Arakawa A, et al. Melanocyte antigen triggers autoimmunity in human psoriasis. J Exp Med. 2015;212(13):2203–2212.
43. Sontheimer RD. Lichenoid tissue reaction/interface dermatitis: clinical and histological perspectives. J Invest Dermatol. 2009;129(5):1088–1099.
44. Vandooren J, Van den Steen PE, Opdenakker G. Biochemistry and molecular biology of gelatinase B or matrix metalloprotein-ase-9 (MMP-9): the next decade. Crit Rev Biochem Mol Biol. 2013;48(3):222–272.
45. Kumar R, Parsad D, Kanwar AJ, Kaul D. Altered levels of Ets-1 transcription factor and matrix metalloproteinases in melano-cytes from patients with vitiligo. Br J Dermatol. 2011;165(2):285–291.

46. Lei TC, Vieira WD, Hearing VJ. In vitro migration of melanoblasts requires matrix metalloproteinase-2: implications to vitiligo therapy by photochemotherapy. Pigment Cell Res. 2002;15(6):426–432.
47. Parks WC, Wilson CL, López-Boado YS. Matrix metalloproteinases as modulators of inflammation and innate immunity. Nat Rev Immunol. 2004;4(8):617–629.
48. Craiglow BG, King BA. Tofacitinib citrate for the treatment of vitiligo: a pathogenesis-directed therapy. JAMA Dermatol. 2015;151(10):1110–1112.
49. Joshipura D, Alomran A, Zancanaro P, Rosmarin D. Treatment of vitiligo with the topical Janus kinase inhibitor ruxolitinib: A
a. week open-label extension study with optional narrow-band ultraviolet B. J Am Acad Dermatol. 2018;78(6):1205–1207.e1.
50. Liu LY, Strassner JP, Refat MA, Harris JE, King BA. Repigmentation in vitiligo using the Janus kinase inhibitor tofacitinib may require concomitant light exposure. J Am Acad Dermatol. 2017;77(4):675–682.e1.
51. Rothstein B, et al. Treatment of vitiligo with the topical Janus kinase inhibitor ruxolitinib. J Am Acad Dermatol. 2017;76(6):1054–1060.e1.
52. Riding RL, Richmond JM, Harris JE. Mouse model for human vitiligo. Curr Protoc Immunol. 2019;124(1):e63.
53. Taïeb A, Picardo M, VETF Members. The definition and assessment of vitiligo: a consensus report of the Vitiligo European Task Force. Pigment Cell Res. 2007;20(1):27–35.
54. Benzekri L, Gauthier Y. Clinical markers of vitiligo activity. J Am Acad Dermatol. 2017;76(5):856–862.
55. Sosa JJ, et al. Confetti-like depigmentation: a potential sign of rapidly progressing vitiligo. J Am Acad Dermatol. 2015;73(2):272–275.
56. Gontier E, et al. Dermal nevus cells from congenital nevi cannot penetrate the dermis in skin reconstructs. Pigment Cell Res. 2002;15(1):41–48.
57. Jacquemin C, et al. Heat shock protein 70 potentiates interferon alpha production by plasmacytoid dendritic cells: relevance for cutaneous lupus and vitiligo pathogenesis. Br J Dermatol. 2017;177(5):1367–1375.